

NIR Reflectance Spectroscopy of Massalia Family Asteroids 8452 Clay, 2316 Jo-Ann, 7760, 52442, 27120 Isabelhawkins. J.T. Germann¹, S. K. Fieber-Beyer^{1,2}, M. J. Gaffey^{1,2}, C. A. Strom¹. ¹Dept. of Space Studies, Box 9008, Univ. North Dakota, Grand Forks, ND 58202. ²Visiting Astronomer at the IRTF under contract from the NASA, which is operated by the Univ. of Hawaii Mauna Kea, HI 97620. jusgermann@gmail.com.

Introduction: The radiometric ³⁹Ar-⁴⁰Ar dating of the L-chondrite meteorites indicate that the L-chondrite parent asteroid underwent a substantial shock event ~470 Ma [1,2]. Furthermore, an inundation of L-chondrite impacts within Ordovician deposits [3–5], and the abundance of L-chondrite falls [6] also indicate that the disrupted parent body’s orbital properties promote efficient fragment delivery to Earth-crossing orbits. As such, we are investigating the Massalia dynamic family as a candidate source for the L-chondrite meteorites because its orbit extends near the 3:1 resonance [7,8], two large members (20 Massalia and 182 Elsa) exhibit spectral parameters consistent with the S(IV) complex [9], its high member count (~6400) [10] and dynamical modeling indicate a relatively young age [8].

Our group is investigating the near-infrared (NIR) spectra of the Massalia family to determine if it is a probable source for the L-chondrites. We are looking at the spectral parameters (BI, BII, BAR) to infer the mineralogic composition of the family as a whole. This current abstract reports the analysis of five dynamical members of the Massalia family.

Data and Methods: Near-infrared spectra of asteroids 2316, 8452, 7760, 52442, and 27120 were obtained using the NASA IRTF SpeX instrument [11] in low resolution mode (0.68-2.54- μ m) in November 2019 and September 2020. Asteroid and standard star observations were interspersed within the same airmass range to allow for modeling of atmospheric extinction. Data reduction was done using previously outlined procedures [12,13].

Results: Table 1 reports the spectral properties of featured asteroids. Table 2 reports the calculated chemistries and possible meteorite analog for each asteroid. Chemistries of ordinary chondrite equivalent asteroids were calculated using [15], while HED equivalent asteroids chemistries were calculated using [16]. Figure 1 shows the reduced spectrum of all five asteroids. Figure 2 is the BI center vs BAR plot used to determine the S-complex type of featured asteroids. Asteroid surface temperatures were calculated using [17]. Temperature corrections were calculated using procedures outlined in [18] for likely OC equivalent asteroids and [19] for likely HED equivalent asteroids.

2316 Jo-Ann: The VNIR spectrum of 2316 was produced by normalizing the SMASS-II spectrum [20] with the observed NIR spectrum. The spectrum of 2316 is featureless with a positive slope that reaches a

maximum reflectance at ~0.65- μ m followed by a negative slope throughout the NIR. 2316 is classified as a C-type [21] and as a Cb-type by [14].

8452 Clay: The spectrum of 8452 exhibits two absorption features (Table 1). Plotting the B1 center vs BAR shows it is consistent with the S(IV) asteroids [9] (Figure 2.). 8452’s chemistry is consistent with H-chondrites (Table 2). [15]. However, our measurements showed a bluer slope when compared to 2MASS photometric observations [22]. This discrepancy could be the result of observing a less weathered surface such as a hemisphere with large intact boulders [23].

7760: The spectrum of 7760 exhibits two strong bands (Table 1). The BI center vs BAR plot is consistent with the HED S-complex [9], and the pyroxene chemistry was calculated [16] and reported in Table 2.

52442: The spectrum of 52442 exhibits two absorption features (Table 1). The high uncertainty of the BAR measurement is caused by excessive noise in the spectrum longward of ~1.8- μ m. The BI center vs BAR is consistent with S(IV) complex [9], and its chemistry is consistent with H-chondrites (Table 2).

27120: The spectrum of 27120 has two measurable bands (Table 1). The high BAR uncertainty is caused by the noisy spectrum longward of ~1.8- μ m. The BI center vs BAR plots outside the S-complex; however, its BAR

Table 1. ‘BI’ and ‘BII’ columns indicate the Band 1 and Band 2 centers. ‘BAR’ is the calculated band area ratio. Reported values are temperature corrected.

Asteroid	BI (μ m)	BII (μ m)	BAR
8452	0.94 \pm 0.01	1.95 \pm 0.04	0.88 \pm 0.05
7760	0.93 \pm 0.01	1.94 \pm 0.02	2.179 \pm 0.16
52442	0.92 \pm 0.01	2.21 \pm 0.03	0.64 \pm 0.28
27120	0.91 \pm 0.01	2.01 \pm 0.03	0.73 \pm 0.60

Table 2. Calculated chemistries and meteorite analog for each featured spectrum. Asteroid’s analogous to chondrites were calculated using [15]. HED analog chemistries were calculated using [16].

Asteroid	Fs	Wo	Fa	Analog
8452	16.9	N/A	19.5	H-OC
7760	31.38	5.30	N/A	HED
52442	15.1	N/A	16.9	H-OC
27120	11.08	N/A	10.97	inconclusive

uncertainty overlaps with the S(VI) region.

Conclusions: 8452 and 52442 have chemistries consistent with H-ordinary chondrites. 27120's Fa and Fs compositions indicates a lack of Fe in silicate minerals. 27120 also has an uncertain S-complex, so possible meteorite analogs could range from the ordinary chondrites, to a primitive Fe-poor meteorite such as siderophyres [9]. 7760 chemistry is equivalent to the HED meteorites [9]. The high noise in 27120's and 52442's spectra was likely due to both objects having visible magnitudes > 17.4 during observations.

None of the observed asteroids are consistent with L-chondrite spectral properties. However, these observations do not indicate that the Massalia family is not a suitable candidate for the L-chondrite source. The five asteroids reported are a small sample of the Massalia member population (~ 6400) [10]. The asteroid belt is a relatively dynamic environment, this is even more true near orbital resonances. Therefore, it is not uncommon for an interloper to be injected into the family's orbit [24]. Therefore, further investigation into the Massalia family population is required before any conclusion of a possible L-chondrite relation can be ascertained.

Acknowledgments: This material is based upon work supported by the National Science Foundation under Grant No. 1841809 (MJG & SFB). We thank the IRTF TAC for awarding time to this project, and to the IRTF TOs and MKSS staff for their support.

References: [1] Korochantseva E. V. et al. (2007) *Meteorit. Planet. Sci. Arch.* 42, 113–130. [2] Heymann D. (1967) *Icarus* 6, 189–221. [3] Schmitz B. et al. (2003) *Science* 300, 961–964. [4] Schmitz B. et al. (2001) *Earth Planet. Sci. Lett.* 194, 1–15. [5] Lindskog A. et al. (2012) *Meteorit. Planet. Sci.* 47, 1274–1290. [6] Keil K. et al. (1994) *Planet. Space Sci.* 42, 1109–1122. [7] Milani A. et al. (2014) *Icarus* 239, 46–73. [8] Vokrouhlický D. et al. (2006) *Icarus* 182, 118–142. [9] Gaffey M. J. et al. (1993) *Icarus* 106, 573–602. [10] Nesvorný D. (2015) *NASA Planet. Data Syst.* [11] Rayner J. T. et al. (2003) *Publ. Astron. Soc. Pac.* 115, 362–382. [12] Gaffey M. (2002) *Asteroids III*, pp. 183–204. [13] Fieber-Beyer S. K. and Gaffey M. J. (2020) *Planet. Sci. J.* 1, 68. [14] Dunn T. L. et al. (2010) *Icarus* 208, 789–797. [15] Burbine T. H. et al. (2001) *Meteorit. Planet. Sci.* 36, 761–781. [16] Burbine T. H. et al. (2009) *Meteorit. Planet. Sci.* 44, 1331–1341. [17] Sanchez J. A. et al. (2012) *Icarus* 220, 36–50. [18] Reddy V. et al. (2012) *Icarus* 217, 153–168. [19] Bus S. and Binzel R. (2003) *NASA Planet. Data Syst.* [20] Bus S. J. (1999) *Mass. Inst. Technol.* [21] DeMeo F. E. et al. (2009) *Icarus* 202, 160–180. [22] Sykes M. V. et al. (2000) *Icarus* 146, 161–175. [23] Lantz C. and Clark B. E. (2012) ... *Planet. Sci. Congr. 2012 Held 23-* ... 7, 3–5. [24] Migliorini F. et al. (1995) *Icarus* 118, 271–291.

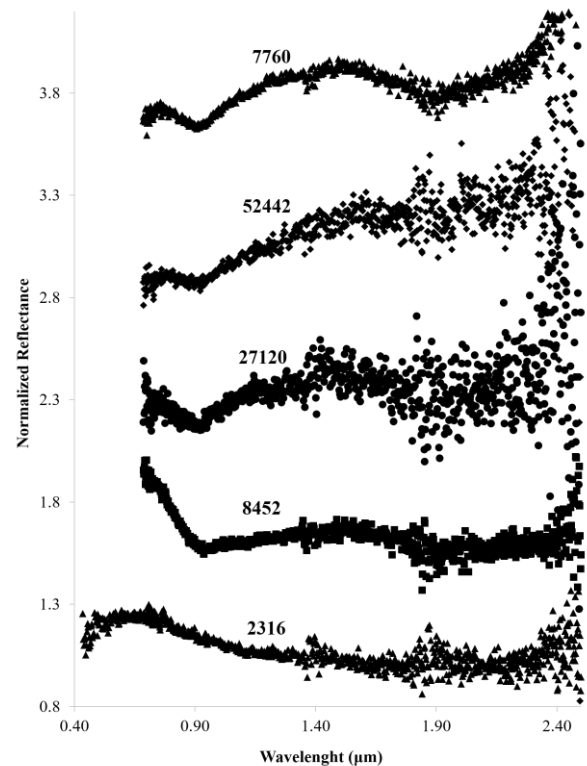


Figure 1. Reduced spectrum of observed asteroids. All but asteroid 2316 had two measurable bands. 8452 and 52442 are consistent with H-chondrites. 27120 may be equivalent to high-opx. 7760 is equivalent to HED's.

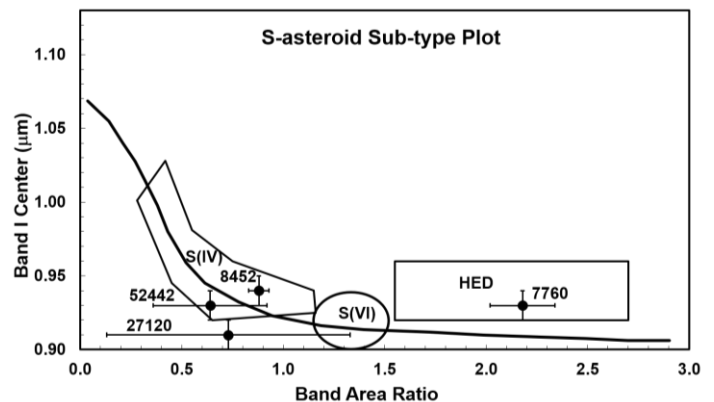


Figure 2. BI Center – BAR plot, relevant S-complex zones are labeled, along with each asteroid. Plot modified from [9].